We are IntechOpen, the world's leading publisher of Open Access books Built by scientists, for scientists

6,900
Open access books available

185,000
International authors and editors

200M
Downloads

Our authors are among the

154
Countries delivered to

TOP 1%
most cited scientists

12.2%
Contributors from top 500 universities

WEB OF SCIENCE™

Selection of our books indexed in the Book Citation Index in Web of Science™ Core Collection (BKCI)

Interested in publishing with us?
Contact book.department@intechopen.com

Numbers displayed above are based on latest data collected.
For more information visit www.intechopen.com

7

Deformable Model-Based Segmentation of Brain Tumor from MR Images

Sami Bourouis and Kamel Hamrouni
University Tunis El-Manar, National Engineering School of Tunis
Tunisia

1. Introduction

Segmentation of brain tumors is an important task for treatment planning and therapy evaluation. This task could also lead to new applications, including data compression, robust registration, and effective content based image retrieval in large medical databases. Accurate delineation of tumor can also be helpful for general modeling of pathological brains and the construction of pathological brain atlases Toga et al. (2001). Nevertheless, precise delineation of brain Tumor in MRI is a challenging problem that depends on many factors. Indeed, there is a large class of tumor types which vary greatly in size and position, have a variety of shape and appearance properties, have intensities overlapping with normal brain tissue, may deform and defect the surrounding structures giving an abnormal geometry also for healthy tissue. Moreover, MR images segmentation widely depends on the specific application and image modality. These images contain sometimes various amounts of noise and/or artifacts due to patient's motion and soft tissue boundaries are sometimes not well defined.
Traditionally manual brain tumors segmentation - usually performed by marking the tumor regions slice-by-slice by human expert - is time-consuming (hence impractical for processing large amounts of data), non- reproducible, difficult, and highly subjective. On the other hand, fully automatic and robust segmentation is highly required for clinical settings because it reduces significantly the computing time and generates satisfactory segmentation results.
The existence of several MR acquisition protocols provides different information on the brain. Each image usually highlights a particular region of the tumor. In visualizing brain tumors, a second T1-weighted image is often acquired after the injection of a 'contrast agent'. These 'contrast agent' usually contain an element whose composition causes a decrease in the T1 time of nearby tissue (gadolinium is one example) Brown & Semeka (2003). The presence of this type of 'enhancing' area can indicate the presence of a tumor. Figure 1 illustrates an example of T1-weighted image before and after the injection of a contrast agent.
Conventionally, it is difficult to segment a tumor by a simple technique like thresholding or classic edge- detection. These methods may not allow differentiation between non-enhancing tumor and normal tissue due to overlapping intensity distributions of healthy tissue with tumor and surrounding edema. Also, they are unable to exploit all information provided by MRI. Therefore, advanced image analysis techniques are needed to solve the problem.
Various promising works have studied the tumor segmentation, offering a diversity of methods and evaluation criteria. In particular, pattern classification techniques refer to a

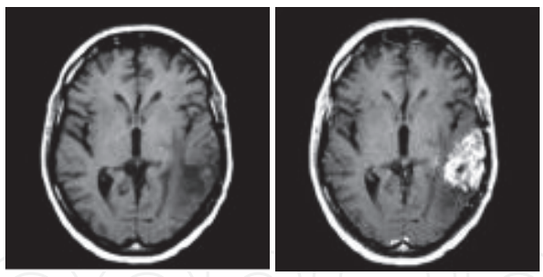

(a) (b)

Fig. 1. Effects of contrast agent. (a): T1-weighted image, (b) T1-weighted image after contrast injection

large class of methods Corso et al. (2008); Liu et al. (2005); Prastawa et al. (2004); Zhang et al. (2001). For example, in a more recent publication, a Bayesian generative model Corso et al. (2008) is applied to brain tumor detection. This model is incorporated into the graph-based image segmentation. Fuzzy-connectedness Liu et al. (2005) and Markov random fields (MRFs) Zhang et al. (2001) are also ones of a useful method for medical image segmentation.

Other approaches were proposed in literature for brain tumor segmentation and the most of them focused on the use of a combinational strategy of several conventional techniques such as : mathematical morphological operations, registration methods, deformable models, anatomical information and voxel-based techniques Cobzas et al. (2007); Cuadra et al. (2004); Moon et al. (2002); Warfield et al. (2000). For instance, Warfield et al. Warfield et al. (2000) have proposed an ATM SVC algorithm that overcomes the limitations of intensity-based classification and Template based non-linear registration techniques by embedding both image and model information into a higher dimensionality space in which a k-Nearest Neighbors (k-NN) classification is performed. Cuadra et al. Cuadra et al. (2004) have presented an efficient tool for pathological brain segmentation. The idea is to deform the atlas in presence of large space-occupying tumors, based on an a priori model of lesion growth. Authors in Cobzas et al. (2007) have proposed a region-based variational method for brain tumor segmentation. They define a set of multidimensional features and use them to calculate statistics for 'tumor' and 'normal brain' area from labeled MRI data.

Many of these published works have been successfully applied to segment some tumor types. However, some of them fail when the ROI to be identified have overlapping spectral properties. It is also too difficult to differentiate between normal and abnormal tissues when dealing with only one modality (such as T1-weighted MR image) because the acquisition of tissue parameters is insufficient due to the lack of contrast. They are also very computationally expensive and the accuracy of the segmentation depends on the initial parameters. For instance, the use of atlas is problematic because tumor structures have no equivalent in the atlas. Moreover, algorithmic complexity is another disadvantages of some approaches cited above.

Deformable models are other popular methods that are widely used for a wide range of applications and have proved to be a successful segmentation technique Bourouis et al. (2008); Liew & Yan (2006). They have become used for medical image processing and especially for brain segmentation, implicitly in the form of a level set function Sethian (1999) or explicitly as a snake function Kass et al. (1987).

In the recent years, the level set method has become popular thanks to its ability to handle complex geometries and topological changes. Unlike the traditional deformable models, the level set method does not depend on the parameterizations of the surface. Moreover, they constitute an appropriate framework for merging heterogeneous information and they provide a consistent geometrical representation suitable for a surface-based analysis. These advantages make level-set technique very attractive and flexible in shape modeling and image segmentation.

A region-based speed function Ho et al. (2002) have been developed for automatic 3D segmentation of brain tumors by combining region based level sets and fuzzy clustering. An initial surface is used to guide an automatic initialization by calculating the difference image of T1-weighed images with and without gadolinium enhancement. The proposed speed function overcomes classical level-set functions by modulating the propagation term with a signed statistical force, leading to a stable solution. However, this method only segments the enhanced section of tumors in contrast enhanced T1-weighted image. A more recent approach was presented in Taheri et al. (2010), combining the threshold-based method and level sets. This method is similar to the method of Chen & Metaxas (2003) but it works in 3D and uses a threshold method to construct the speed function in level sets. The algorithm is started by selecting one or several ROI in the tumor region. An initial threshold value is calculated using these ROIs and a level set with the proposed threshold-based speed function is deformed using ROI(s) as zero level set. A semi-automatic algorithm in Bourouis & Hamrouni (2010) was applied to delineate tumor volume based on deformable model approach. Authors proposed a new function speed modulated by both boundary and regional information in order to have a more robust process for segmentation.

Unfortunately, there are difficulties in using level sets. One problem is that level set algorithm requires accurate initialization and robust attraction force to converge successfully. Another problem is that level set formulation needs the updating of several parameters. The main parameter in the level set equation is the speed function, whose design is the most important step in the level set approach. Consequently, this approach becomes less desirable in some circumstances.

In general, precise and reproducible segmentation of brain tumors are still a challenging and difficult task which is far from being solved, even if much effort has been spent in the medical imaging community.

As with most other works, we focus on the development of a generic algorithm that could help in the automation of medical image analysis tasks. Our work takes place in this growing area and we are mainly motivated by the deformable model approaches. This chapter extends some works and proposes an unsupervised method that incorporates additional information to better disambiguate the tumor from the surrounding deformed brain tissue. Unlike our previous method Bourouis & Hamrouni (2010), we propose here a fully automatic and more robust procedure for tumor segmentation.

2. Brief mathematical formulation of level sets

In the present section we provide a brief overview of some of the requisite mathematics that are needed to understand level-set technique. While detailed proofs are not included, the interested reader can refer to citations and detailed descriptions in Osher & Sethian (1988); Sethian (1999).

The level set method, developed by Osher and Sethian Osher & Sethian (1988), is an emerging method to represent shapes and track moving interfaces. The basic idea is to change the movement of a planar curve into the movement track of 3D surface.
Theoretically, the level set boundary is defined as a zero level set of an implicit representation ϕ of an evolving front $\Gamma(t)$. The implicit level set function ϕ can be evolved by solving the following PDE (partial differential equations) :

$$\frac{\partial \phi}{\partial t} = F.|\nabla \phi| \tag{1}$$

Where F is a scalar velocity (speed) function depending on the local geometric properties (e.g curvature) and on the external parameters related to the input data (e.g image gradient). ∇ denotes the gradient operator. The speed function F may be expressed as $F = F(k)$, where the local curvature k is given by:

$$k = div(\frac{\nabla \phi}{|\nabla \phi|}) = \nabla.\frac{\nabla \phi}{|\nabla \phi|} = \frac{\phi_{xx}\phi_y^2 - 2\phi_x\phi_y\phi_{xy} + \phi_{yy}\phi_x^2}{(\phi_x^2 + \phi_y^2)^{\frac{3}{2}}} \tag{2}$$

At time t the zero level set ($\phi = 0$) describes the evolved of front. Thereby, $\Gamma(t)$ (see Figure 2) deforms iteratively according to its normal direction with the speed function F, and its position is given at each iteration step by the equation:

$$\Gamma(x, y, t) = \{(x, y)/\phi(x, y, t) = 0\} \tag{3}$$

The initial function ϕ_0 is calculated based on the signed measure to the initial front Γ_0. It can be simply the Euclidean distance between one image point and the boundary the front. That is:

$$\phi_0(x, y) = \pm d((x, y), \Gamma_0) \tag{4}$$

The sign of the distance $d(x, y), \Gamma_0)$ is chosen such that the point inside the boundary has a negative sign and the one outside has a positive sign.

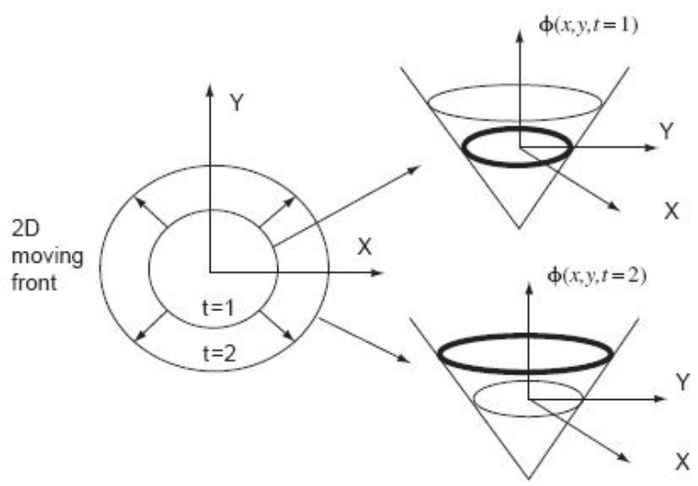

Fig. 2. The level set function.

For image segmentation purposes and in order to solve the shape recovery problem, Malladi et al. Malladi et al. (1995) and Caselles et al. Caselles et al. (1997) have introduced two kinds of speed functions, among others. To stop the evolution at the edge, F can be multiplied by a value that is a function of the image gradient Malladi et al. (1995). However, if the edge is missed, the surface cannot propagate backward. Hence, relying mainly on the edge is not sufficient for an accurate segmentation and other information from image should be used.
Because the initialization of the model through Eq. (2) is computationally expensive, there is an efficient way to solve the initial value of the level set problem: The Narrow Band method Sethian (1999). The key idea of this technique is to constrain the computation only to the pixels that are close to the zero level set. Therefore, by performing a narrow band update of the level set, we need only construct the speed function at a small set of points in the neighborhood close to the zero level set instead of constructing it at all the points on the image domain. We present below the basic pseudo-code of the Narrow-Band, and readers are referred to Sethian (1999) for details.

1. Initialize the signed distance function ϕ_0 of the initial front Γ_0,
2. Find the narrow band points: determine those points whose distance $|\phi(t)|$ is less than the specified narrow bandwidth, and mark them as the narrow band points,
3. Update: resolve level set equation, and track the zero level set curve; update the level set function value $|\phi(t + \Delta t)|$ in the narrow band,
4. Reinitialize: reinitialize the narrow band when the zero level set reaches the boundary of the narrow band. Repeat steps 3 and 4.
5. Convergence test: check whether the iteration converges or not. If so, stop; otherwise, enter the calculation of the next step, and go to step 3.

3. Methods and materials: Tumor segmentation

Our aim is to provide a stable and accurate solution for the segmentation of brain tumor. In this work, we propose two procedures for tumor segmentation: the first is a semi-automatic algorithm whereas the second is completely automatic.

3.1 Semi-automatic algorithm : single modality image

At this stage, we propose an algorithm (Algorithm: 1) that is able to detect tumor volume with a semi-automatic method based mainly on a partial derivative equation described below. Indeed, the user initializes the algorithm by manually selecting one voxel (we need only the position of the seed point) which belongs to the tumor area. This process could lead to generate the initial deformable model for the tumor area. Hence, this first model is defined as a set of neighbor's voxels having the same of intensity properties with the selected voxel. In the following stage, the initial deformable model will be deformed until extracting all tumor region.
The different steps of the current algorithm are summarized as follows:

3.2 Fully automatic algorithm : multimodality images

The fully automatic segmentation process is often a necessary task for medical applications. However, it has been proven to be problematic, both due to the high complexity of anatomical structures as well as their large variability. We think that it would be possible to automate our

Algorithm 1

1. Preprocessing step: Volume smoothing.

2. Manual selection of an initial voxel v_T.

3. Initial model estimation for tumor area: a set of neighbor's voxels $\vartheta(v_T)$ define this model ; calculation the mean value m_T in order to initialize the evolution of the deformable model.

4. Segmentation of the tumor under the action of the evolving level-set equation.
   - Taking into some evolution constraints (such as epsilon parameter ϵ_T and the maximum number of iterations).

method if we take account of more of MRI images such as weighted pre- and post-contrast 3D images. Indeed, the injection of gadolinium is used to differentiate tumor contrast from other close tissues. Under these conditions, we propose to use for example the same idea which was developed by other researchers such as Ho et al. Ho et al. (2002).
Operations performed by the current algorithm are summarized in figure 3.

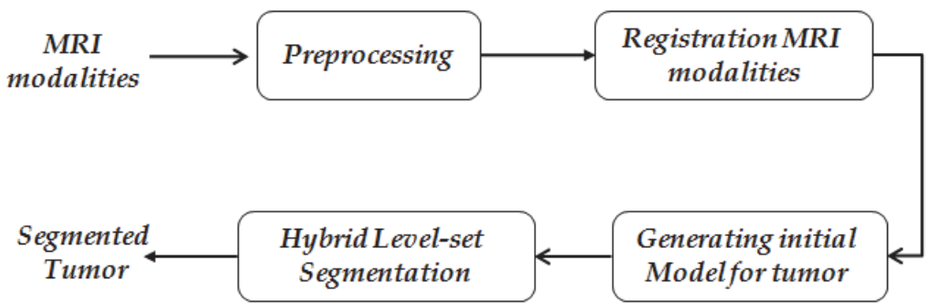

Fig. 3. The proposed algorithm.

Preprocessing step: (Smoothing and Edge Preserving)
We perform a pre-processing step that reduces the effect of noise and intensity variations within and between images. Here we use an anisotropic diffusion filter Perona & Malik (1990), which can remove only high-frequency noise, preserve edge, and should not affect relevant major geometrical features.

Affine registration step:
An alignment of different modalities is carried out using mutual information criterionMaes et al. (1997) to globally match different MRI modalities.

Initialisation step:
The aim of this step is to create an initial model that must be able to derive an automatic initialization of the surface and to locally guide the level set surface.

Level-Set evolution step:
The intention of this step is to extract accurately brain tumor volume by applying an efficient deformable model. As the evolution process can be guided by a combination of several information, we propose here an hybrid framework which controlled by a new evolution speed function. This function is able to take into account simultaneously the local spatial context and the global one. This mechanism may lead the algorithm to a stable and precise solution.

3.2.1 Initialization step

T1-weighted pre- and post-contrast 3D images are the inputs to perform an automatic initialization for our procedure. The use of T1-weighted pre- and post-contrast shows different aspects of the tumor region. T1-weighted MRI is commonly used for detailed imaging of anatomy, but do not distinguish tumor tissue well. At this stage, we calculate the difference image of T1-weighed images with and without contrast enhancement. This initial map is then used to derive an automatic initialization of the surface and to locally guide the level set surface. However, the obtained difference image from the last operation includes tumor voxels and some normal tissues. As we need only pathological voxels to initialize the level-set function, we apply a post-processing based on mathematical morphology operations. A binary morphological erosion process is applied to eliminate noise as well as normal tissue structures while retaining the brain tumor areas. This process requires the definition of the radius size of the neighbourhood associated with the structuring element. Finally, the mean and epsilon values of the obtained tumor area are calculated in order to start the evolution of the deformable model with the best parameters.

3.2.2 Adaptive, hybrid level-set evolution

In this section we detail the second step of the proposed approach: the previous detection of the tumor is used to initialize a deformable model.
Construction of a speed function is crucial in applying the level set method to medical image segmentation. The speed function is designed to control movement of the curve. In this section we focus on the construction of a novel speed function. Our intention is to exploit the advantage of the combination/cooperation of different information in the same framework. So, we propose basically to constrain our deformable model by both boundary and regional information.
To speed up the implemented algorithm, we propose the use of Narrow Band Sethian (1999). We remember that the contour of an object is defined as the zero level set of an implicit function ϕ. This function will change with time according to the evolution force F.
The partial differential equationSethian (1999) of ϕ is defined as follows:

$$\frac{\partial \phi}{\partial t} = F|\nabla \phi| \tag{5}$$

The classical evolution force is defined like in Malladi et al. (1995):

$$F = g(I)(\nu + k) \tag{6}$$

Where the curvature k and the constant force ν propagate the curve to image edges. $g(x)$ is a stopping function that limits the propagation force at edges.

The design of the velocity F plays a major role in the evolutionary process. Recently Bourouis & Hamrouni (2010), we have proposed the following formulation for the evolution equation (7):

$$\frac{\partial \phi}{\partial t} = [\alpha_r F_{region}(I) + \alpha_b F_{boundary}(I)]|\nabla \phi| \tag{7}$$

Where F_{region} and $F_{boundary}$ define the propagation term.
F_{region} is a region-based propagation term and $F_{boundary}$ is a boundary-based term. These two terms force the model to expand or contract toward desirable features in the input data. The constants α_r and α_b control the degree of evolution and smoothness in the solution.
$F_{boundary}$ causes the evolving of the front to be more strongly attracted to image edges. It is expressed as :

$$F_{boundary}(I) = sign(F_{boundary}).\frac{c+k}{1+|\nabla I|} \tag{8}$$

$$sign(F_{boundary}) = \begin{cases} +1 \; if & F_{region} < 0 \\ -1 \; otherwise & \end{cases} \tag{9}$$

The curvature k forces the surface to have smooth area.
F_{region} controls the evolution of the model and segments tumor tissue based on intensity values. We define F_{region} as:

$$F_{region}(I) = \begin{cases} I - (m_T - \epsilon_T) \text{ if } I < m_T \\ (m_T + \epsilon_T) - I \text{ otherwise} \end{cases} \tag{10}$$

Where ϵ_T is a constant parameter, and m_T is the mean value of the tumor region.
ϵ_T controls the brightness of the region to be segmented and define a range of greyscale values that could be considered inside the object.
In this way a model situated on voxels with greyscale values in the interval $[m_T - \epsilon_T, m_T + \epsilon_T]$ will expand to enclose that voxel, whereas a model situated on greyscale values outside that interval will contract to exclude that voxel. So, intensity values between $m_T - \epsilon_T$ and $m_T + \epsilon_T$ yield positive values in F_{region} (i.e the model expands), while outside intensities yield negative values in F_{region} (i.e the model contracts).
Finally, the algorithm will stop if the maximum number of iterations is terminated or if the convergence criterion is reached. The convergence criterion is defined in terms of the root mean squared error (RMSE). If the maximum RMSE value is reached, the solution is considered to have converged.

$$RMSE = \sqrt{\frac{1}{N \times M} \sum_{i=1}^{N} \sum_{j=1}^{M} (\phi_{i,j}^{n+1} - \phi_{i,j}^{n})^2}$$

Wher $N \times M$ is the matrix size of ϕ and $\mathbf{n}$ indicates the n^{th} iteration.

In this work, we propose to improve our previous deformable model by introducing new parameters which help the evolution stability. More details will be introduced in the next section.

3.2.3 Threshold updating parameter

To improve the performance of the level set equation, we propose to change our previous region-based speed function (eq. 10) by an adaptive scheme which is better than the static one. This idea was already proposed by Taheri et al. Taheri et al. (2010).

Modified Region-based speed Function :

We introduce the bellow modifications to redefine the region speed term in order to segment also "non-homogeneous" tumor tissues. So, we propose to define a threshold updating parameter τ as:

$$\begin{cases} \epsilon_T = \sigma_T \\ \tau^{i+1} = m_T^i - sign(I).k.\sigma_T^i \end{cases} \tag{11}$$

Where

$$sign(x) = \begin{cases} +1 \text{ if } x < m_T^i \\ -1 \text{ otherwise} \end{cases} \tag{12}$$

τ^{i+1} : the threshold estimation for the (i+1)th iteration.
m_T^i : the mean value of the tumor region.
σ_T^i : the standard deviation of the tumor region.
k : is the factor which determines the confidence level and must be chosen properly.

The new formulation for the region-based speed term will define as:

$$\widetilde{F}_{region}^{i+1}(I) = \begin{cases} I - \tau^{i+1} \text{ if } I < m_T^i \\ \tau^{i+1} - I \text{ otherwise} \end{cases} = \begin{cases} I - (m_T^i - k.\sigma_T^i) \text{ if } I < m_T^i \\ (m_T^i + k.\sigma_T^i) - I \text{ otherwise} \end{cases} \tag{13}$$

At each iteration, the mean value m_T^i and the standard deviation σ_T^i are updating according to the equations below:

$$m_T^i = \frac{1}{n}\sum_{j=1}^{n} x_j \qquad \sigma_T^i = \frac{1}{n-1}\sum_{j=1}^{n}(x_j - m_T^i)^2 \tag{14}$$

Where n is the number of accepted tumor samples $\{x_j\}$.
The convergence of the algorithm is related to the choice of τ and k. Indeed, for a small value of k, the level set may never grow while for a relatively large value of k, convergence may not be possible.

4. Validation

The brain tumor MR images used in this work were generated by the simulator: *Simulated Brain Tumor MRI Database* Prastawa et al. (2009). The main advantage of these simulations is the existence of ground truth about the true tumor extent (in form of probability maps for the distribution of tumor and edema). We used five volumes: each volumetric image contained 256 x 256 x 181 voxels. Moreover, Three different imaging modalities (T1-weighted with and without gadolinium enhancement and T2-weighted) are provided.

Our experimental MRI data consists of T1 and T1w (T1 after injection with contrast agent - gadolinium). To evaluate the segmentation results, we compute the similarity index known as the kappa statistics (Dice similarity coefficient that is equivalent to Jaccard similarity measure) Zijdenbos et al. (1994a). It measures the normalized intersection in voxel space of two segmentations: in general the manual segmentation (GT) (Ground Truth) and another one (S). This metric is formulated as following:

$$KI = \frac{2|GT \cap S|}{|GT| + |S|} \tag{15}$$

Where $|.|$ is the cardinal of the segmentation result. The operator $\cap$ represents the intersection of two sets. This metric gives a score of 1 for perfect agreement and 0 for complete disagreement. Zijdenbos et al. Zijdenbos et al. (1994b) state that any value of KI above 0.7 indicates a strong agreement.

It should be noted that the overlap measure depends on the size and the shape complexity of the object. On the other hand, It is sensitive to the difference between two sets since both denominator and numerator change with increase or decrease in the overlap. Thus, we also computed error measures by using another metric called "Hausdorff distance". This second metric (HD) represents the maximum surface distance measure, which measures the largest difference between two tumor volumes. It defines the maximum surface distance as :

$$HD = \max(h(S, GT), h(GT, S)) \tag{16}$$

Where

$$h(S, GT) = \max_{x \in S} \min_{y \in GT} |x - y| \tag{17}$$

Some obtained results are given in figure 4 showing the initialization step. Indeed, the first and the second columns of this figure includes T1-weighted image before and after contrast injection. The third column presents the obtained contrast absolute difference images and the last column shows the effect of binary morphological erosion operator (i.e: initial model for the tumor region).

Concerning segmentation step, some segmented tumors are given in figure 6. Indeed, the first column includes T1-weighted image befor contrast injection, the second column shows the extraction of tumor boudaries and the third column shows the comparison between our segmentation (red color) and the ground truth (green color).

From a global point of view, we observed that the contours of the automated segmentations closely follow those of the ground truth labels as shown in figure 6. This observation can be explained by the merging of different source of information in the evolving model and the performing of a post-processing step that refine the segmentation result. Following these experiments, we can deduce that the obtained results are qualitatively strongly acceptable compared to the ground truth.

Quantitative segmentation results, which are performed on some data sets, are also given in Table 1. As we can see in this table, the results for the kappa measure (KI) indicate that the segmentation is reliable.

However, we have noticed some poor results in some cases. For example, it should be noted that the large values of HD in some cases is due to the presence of outliers. This observation can be explained also by the poor image quality, the complexity of the tumor shapes, and the

effect of the τ (threshold estimation) and the smoothness parameter on the level set speed function.

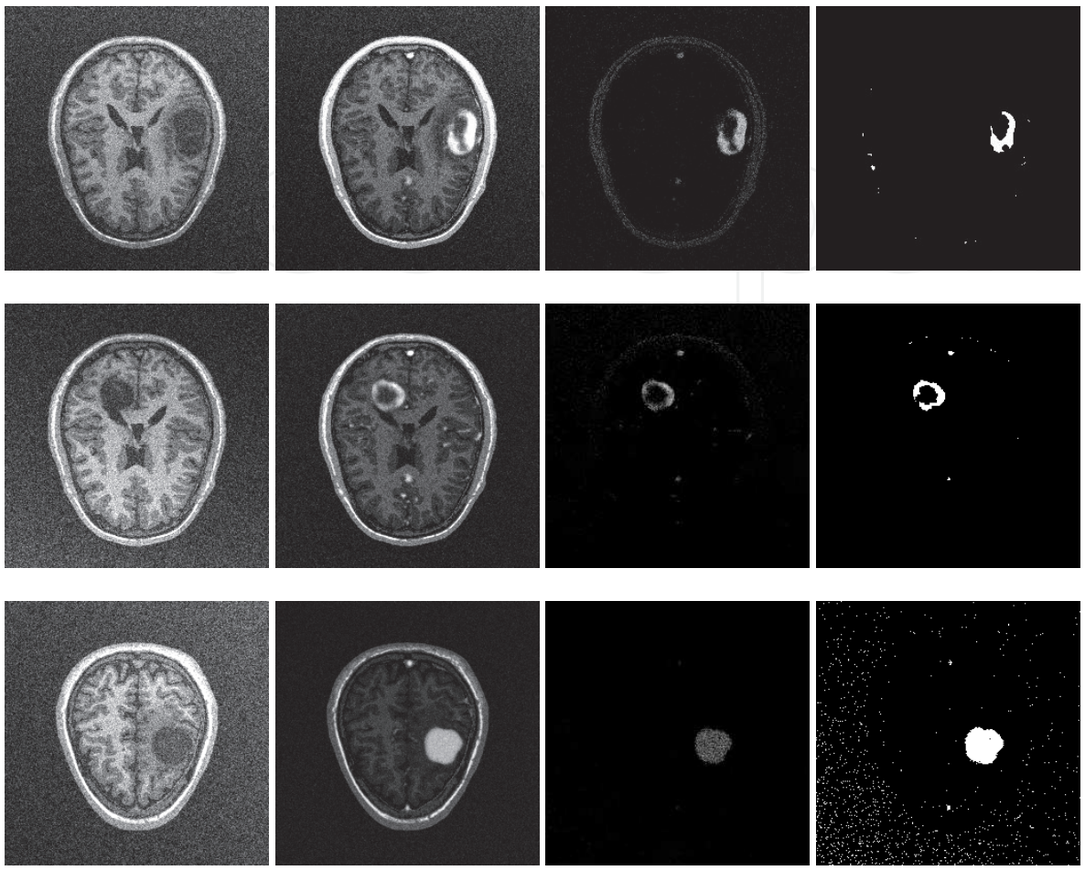

Fig. 4. Active model initialization : The first column includes T1-weighted image. The second column shows T1-weighted image after contrast injection. The third column are contrast absolute difference images. The last column shows the effect of binary morphological erosion operator (i.e: initial model for the tumor region)

Volume	KI (%)	HD (mm)
SimTumor001_Slice090	76,4	9.434
SimTumor001_Slice122	77,5	9.055
SimTumor001_Slice180	83,1	8.062
SimTumor002_Slice090	83,8	5.00
SimTumor002_Slice171	80,2	6.708

Table 1. Kappa measure and Hausdorff distance obtained on some brain tumor scans.

At this stage, the obtained image from the last operation includes a tumor, some tissues with intensities as high as the tumor voxels, and some noisy structures. However, only pathological voxels are needed. For this purpose, we apply a post-processing based on mathematical morphology operations. A binary morphological erosion and dilation process is applied to eliminate noise as well as normal tissue structures while retaining the brain tumor areas.

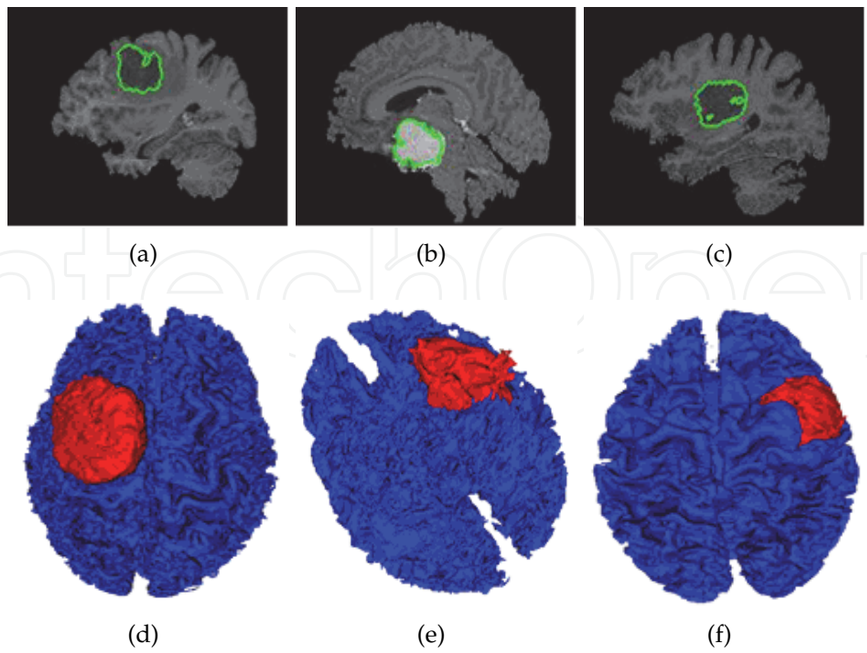

(a) (b) (c)

(d) (e) (f)

Fig. 5. 3D visualization of some tumors (red) within the cerebral cortex (blue). These results are obtained by the semi-automatic algorithm on real T1-weighted MR images

This process requires the definition of the radius size of the neighborhood associated with the structuring element. Once this process is done, we move to the next step to initialize the active model and to refine more and more the segmented tumor area.
We note that we have tested our method on some other real MRI images. Some 3D obtained results are given in figure 5. This figure shows the obtained 3D tumor surface which is superposed on 3D gray matter surface. Indeed, once isolated, the detected tumor can be further processed for volume measurement and three-dimensional rendering.
The mean computation time for the segmentation of a complete 3D image volume takes approximately 3 minutes on a Windows environment with a 2.8 GHz CPU and 512 MB RAM. The algorithm is implemented with C++ language.

5. Summary and discussion

The automatic brain tumor segmentation is an important problem in medical imaging. Although much effort has been spent on finding a good solution to this problem, it is far from being solved.
This chapter surveyed existing methods for brain tumor segmentation in MRI. It presents also a new deformable model based on level-set concept for 3D tumor segmentation. Our proposed deformable model uses both boundary and regional information to define the speed function. We have also proposed a fully automatic initialization process to start our algorithm by considering images with and without contrast enhancement. The segmentation quality in the borders of tumor is relatively good due to the combination of local and global information. Some issues are discussed in this section, including the influence of different parameters on the final segmentation results.

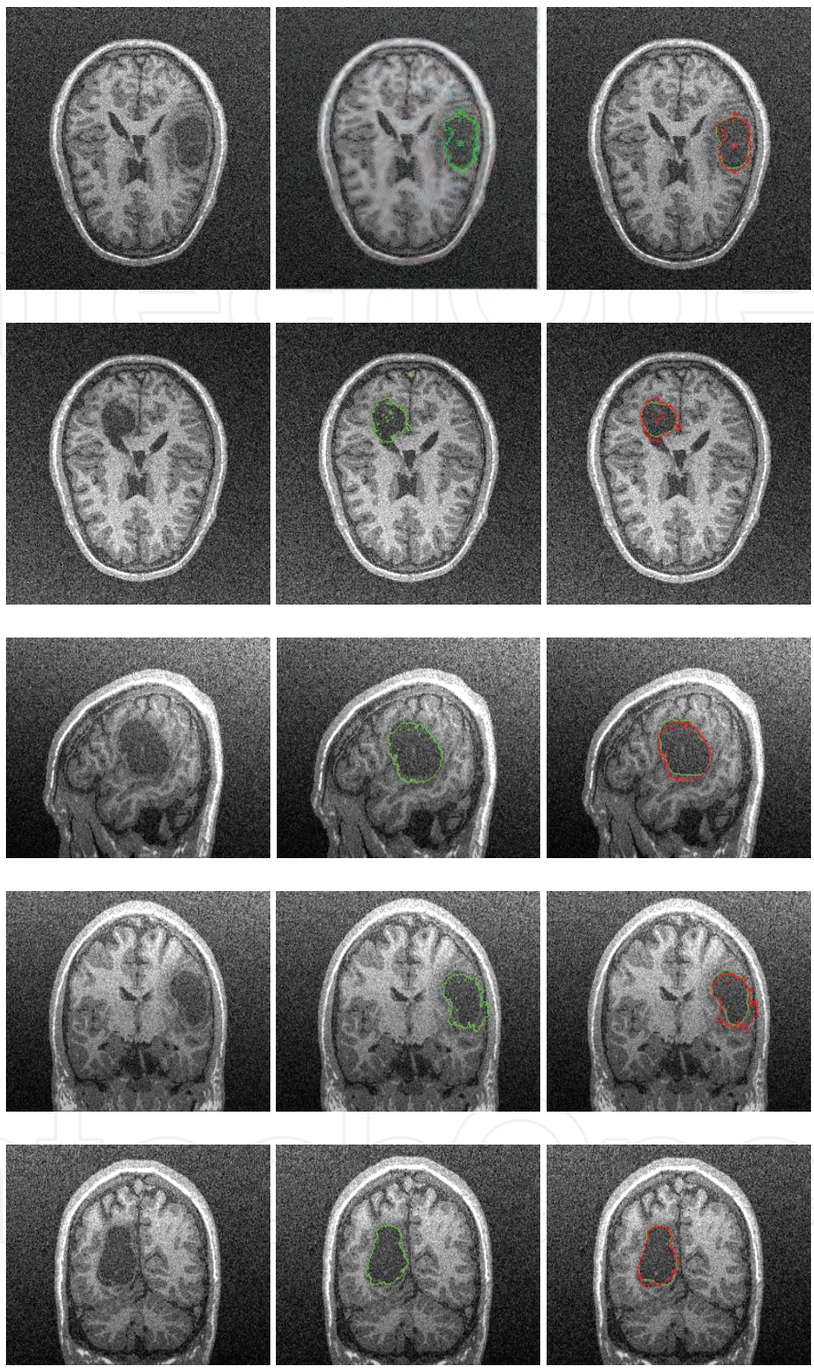

Fig. 6. Brain tumor segmentation: The cross-sections of extracted tumor surfaces with some of their image slices. The first column includes T1-weighted image befor contrast injection. The second column shows the extraction of tumor boudaries. The third column shows the comparison between our segmentation (red color) and the ground truth (green color).

- First of all, the purpose of the proposed method is to surmount limitations of some mentioned methods in the section 1 (Introduction). In particular, it tried to overcome the problem of quality, stability, precision, and to propose an automatic process for segmentation. This is done by the combination of regional and boundary information into the same deformable model formalism. However, the current work can not overcome all limitations and there are improvements to do in our future work.
- In the present study, we didn't consider the influence of non-brain tissue removal, the bias field correction and the partial volume averaging. However, these steps should be considered to avoid possible problems. For example, the brain volume could be extracted by removing the skull by using one of the best known method such as the "Brain Extraction Tool (BET)" Smith (2002).
- Unfortunately, only syntetic tumor types have been considered in this paper. Therefore, the method should be tested on more real data sets containing different kind and size of lesions in order to better validate. Also, further investigations are required to present the effect of tumor size, color, and location.
- Although the presence of this 'enhancement' can be a strong indicator of tumor location, there exist a large variety of types of brain tumors, and their appearance in MR images can vary considerably.

Although the presence of this 'enhancement' can be a strong indicator of tumor location, there exist a large variety of types of brain tumors, and their appearance in MR images can vary considerably.

6. References

Bourouis, S. & Hamrouni, K. (2010). 3d segmentation of mri brain using level set and unsupervised classification, *International Journal in Image and Graphics (IJIG)* Vol. 10(No. 1): 135–154.

Bourouis, S., Hamrouni, K. & Betrouni, N. (2008). Automatic mri brain segmentation with combined atlas-based classification and level-set approach, *5th International Conference on Image Analysis and Recognition, ICIAR,LNCS(5112)* pp. 770–778.

Brown, M. & Semeka, R. (2003). *MRI: Basic Principles and Applications*, John Wiley and Sons, Inc., 3rd edition.

Caselles, V., Kimmel, R. & Sapiro, G. (1997). Geodesic active contours, *International Journal on Computer Vision* Vol. 22(No. 1): 61–97.

Chen, T. & Metaxas, D. (2003). Gibbs prior models, marching cubes, and deformable models: A hybrid framework for 3d medical image segmentation, *Medical Image Computing and Computer-Assisted Intervention (MICCAI)* Springer LNCS 2879: 703–710.

Cobzas, D., Birkbeck, N., Schmidt, M., Jagersand, M. & Murtha, A. (2007). A 3d variational brain tumor segmentation using a high dimensional feature set, *IEEE 11th International Conference on Computer Vision (ICCV)* pp. 1–8.

Corso, J., Sharon, E., Dube, S., El-Saden, S., Sinha, U. & Yuille, A. (2008). Efficient multilevel brain tumor segmentation with integrated bayesian model classification, *IEEE Transactions on Medical Imaging* Vol. 27(No. 5): 629–640.

Cuadra, M., Pollo, C., Bardera, A., Cuisenaire, O., Villemure, J. & Thiran, J. (2004). Atlas-based segmentation of pathological mr brain using a model of lesion growth, *IEEE Transactions on Medical Imaging* 23: 1301–1314.

Ho, S., Bullitt, E. & Gerig, G. (2002). Level set evolution with region competition: Automatic 3-d segmentation of brain tumors, *International Conf on Pattern Recognition ICPR* Vol. 20(No. 8): 532–535.

Kass, M., Witkin, A. & Terzopoulos, D. (1987). Snakes: Active contour models, *Int. J. Comput. Vis.* Vol. 1: 321–331.

Liew, A. & Yan, H. (2006). Current methods in the automatic tissue segmentation of 3d magnetic resonance brain images, *Current Medical Imaging Reviews* Vol. 2: 91–103.

Liu, J., Udupa, J., Odhner, D., Hackney, D. & Moonis, G. (2005). A system for brain tumor volume estimation via mr imaging and fuzzy connectedness, *Computerized Medical Imaging and Graphics* Vol. 29(No. 1): 21–34.

Maes, F., Collignon, A., Meulen, D., Marchal, G. & Suetens, P. (1997). Multi-modality image registration by maximization of mutual information, *IEEE Trans. on Med. Imaging* Vol. 16: 187–198.

Malladi, R., RC., J. S. & Vemuri (1995). Shape modeling with front propagation: A level set approach, *IEEE Trans. Pattern Anal. Machine Intell* Vol. 17(No. 2): 158–174.

Moon, N., Bullitt, E., Leemput, V. & Gerig, G. (2002). Automatic brain and tumor segmentation, *MICCAI* pp. 372–379.

Osher, S. & Sethian, J. (1988). Fronts propagating with curvature-dependent speed: Algorithms based on Hamilton-Jacobi formulations, *Journal of Computational Physics* Vol. 79: 12–49.

Perona, P. & Malik, J. (1990). Scale-space and edge detection using anisotropic diffusion, *IEEE Trans. Med. Imaging* 12: 629–639.

Prastawa, M., Bullitt, E. & Gerig, G. (2009). Simulation of brain tumors in mr images for evaluation of segmentation efficacy, *Medical Image Analysis (MedIA)* Vol. 13(No. 2): 297–311.

Prastawa, M., Bullitt, E., Ho, S. & Gerig, G. (2004). A brain tumor segmentation framework based on outlier detection, *Medical Image Analysis (MedIA)* Vol. 8: 275–283.

Sethian, J. (1999). *Level Set Methods and Fast Marching Methods: Evolving Interfaces in Geometry, Fluid Mechanics, Computer Vision, and Materials Science*, second ed., Cambridge University Press, Place of publication.

Smith, S. (2002). Robust automated brain extraction, *Human Brain Mapping* Vol. 17: 143–155.

Taheri, S., Ong, S. & Chong, V. (2010). Level-set segmentation of brain tumors using a threshold-based speed function, *Image and Vision Computing* Vol. 28: 26Ű–37.

Toga, W., Thompson, A., Mega, P., Narr, M., KL. & Blanton, R. (2001). Probabilistic approaches for atlasing normal and disease-specific brain variability, *Anatomy and Embryology* Vol. 204(No. 4): 267–282.

Warfield, S., Kaus, M., Jolesz, F. & Kikinis, R. (2000). Adaptive, template moderated, spatially varying statistical classification, *Med Image Anal* Vol. 4: 43–55.

Zhang, Y., Brady, M. & Smith, S. (2001). Segmentation of brain mr images through a hidden markov random field model and the expectation-maximization algorithm, *IEEE Transactions on Medical Imaging* Vol. 20: 45–57.

Zijdenbos, A., Dawant, B., Margolin, R. & Palmer, A. (1994a). Morphometric analysis of white matter lesions in mr images: Method and validation, *IEEE Trans. on Medical Imaging* Vol. 13(No. 4): 716–724.

Zijdenbos, A., Dawant, B., Margolin, R. & Palmer, A. (1994b). Morphometric analysis of white matter lesions in mr images: Method and validation, *IEEE Trans. on Medical Imaging* 13(4): 716–724.

IntechOpen

IntechOpen

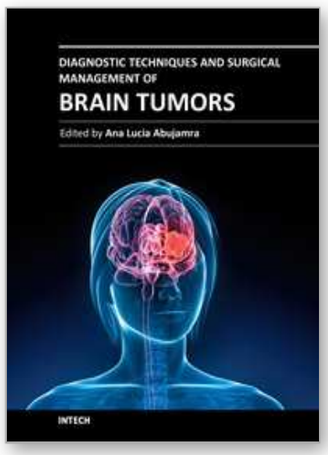

Diagnostic Techniques and Surgical Management of Brain Tumors
Edited by Dr. Ana Lucia Abujamra

ISBN 978-953-307-589-1
Hard cover, 544 pages
Publisher InTech
Published online 22, September, 2011
Published in print edition September, 2011

The focus of the book Diagnostic Techniques and Surgical Management of Brain Tumors is on describing the established and newly-arising techniques to diagnose central nervous system tumors, with a special focus on neuroimaging, followed by a discussion on the neurosurgical guidelines and techniques to manage and treat this disease. Each chapter in the Diagnostic Techniques and Surgical Management of Brain Tumors is authored by international experts with extensive experience in the areas covered.

How to reference
In order to correctly reference this scholarly work, feel free to copy and paste the following:

Sami Bourouis and Kamel Hamrouni (2011). Deformable Model-Based Segmentation of Brain Tumor from MR Images, Diagnostic Techniques and Surgical Management of Brain Tumors, Dr. Ana Lucia Abujamra (Ed.), ISBN: 978-953-307-589-1, InTech, Available from: http://www.intechopen.com/books/diagnostic-techniques-and-surgical-management-of-brain-tumors/deformable-model-based-segmentation-of-brain-tumor-from-mr-images

INTECH
open science | open minds

InTech Europe
University Campus STeP Ri
Slavka Krautzeka 83/A
51000 Rijeka, Croatia
Phone: +385 (51) 770 447
Fax: +385 (51) 686 166
www.intechopen.com

InTech China
Unit 405, Office Block, Hotel Equatorial Shanghai
No.65, Yan An Road (West), Shanghai, 200040, China
中国上海市延安西路65号上海国际贵都大饭店办公楼405单元
Phone: +86-21-62489820
Fax: +86-21-62489821

© 2011 The Author(s). Licensee IntechOpen. This chapter is distributed under the terms of the Creative Commons Attribution-NonCommercial-ShareAlike-3.0 License, which permits use, distribution and reproduction for non-commercial purposes, provided the original is properly cited and derivative works building on this content are distributed under the same license.

IntechOpen

IntechOpen